

# Impact of Acute Pulmonary Embolization on Arterial Stiffening and Right Ventricular Function in Dogs

ALESSANDRO BELLOFIORE,<sup>1</sup> ALEJANDRO ROLDÁN-ALZATE,<sup>2</sup> MATTHIEU BESSE,<sup>1</sup> HEIDI B. KELLIHAN,<sup>3</sup>  
DANIEL W. CONSIGNY,<sup>2</sup> CHRISTOPHER J. FRANCOIS,<sup>2</sup> and NAOMI C. CHESLER<sup>4</sup>

<sup>1</sup>Department of Biomedical Engineering, University of Wisconsin-Madison, 1550 Engineering Drive, Madison, WI 53706-1609, USA; <sup>2</sup>Department of Radiology, University of Wisconsin-Madison, 600 Highland Avenue, Madison, WI 53792-3252, USA;

<sup>3</sup>School of Veterinary Medicine, University of Wisconsin-Madison, 2015 Linden Drive, Madison, WI 53706-1102, USA; and

<sup>4</sup>Department of Biomedical Engineering, University of Wisconsin-Madison, 2146 Engineering Centers Building, 1550 Engineering Drive, Madison, WI 53706-1609, USA

(Received 3 May 2012; accepted 21 July 2012; published online 4 August 2012)

Associate Editor Ender A. Finol oversaw the review of this article.

**Abstract**—Pulmonary hypertension (PH) can impact right ventricular (RV) function and alter pulmonary artery (PA) stiffness. The response of the RV to an acute increase in pulmonary pressure is unclear. In addition, the relation between total pulmonary arterial compliance and local PA stiffness has not been investigated. We used a combination of right heart catheterization (RHC) and magnetic resonance imaging (MRI) to assess PA stiffening and RV function in dogs before and after acute embolization. We hypothesized that in moderate, acute PH the RV is able to compensate for increased afterload, maintaining adequate coupling. Also, we hypothesized that in the absence of PA remodeling the relative area change in the proximal PA (RAC, a noninvasive index of local area strain) correlates with the total arterial compliance (stroke volume-to-pulse pressure ratio). Our results indicate that, after embolization, RV function is able to accommodate the demand for increased stroke work without uncoupling, albeit at the expense of a reduction of efficiency. In this acute model, RAC showed excellent correlation with total arterial compliance. We used this correlation to assess PA pulse pressure (PP) from noninvasive MRI measurements of stroke volume and RAC. We demonstrated that in acute pulmonary embolism MRI estimates of PP are remarkably close to measurements from RHC. These results, if confirmed in chronic PH and clinically, suggest that monitoring of PH progression by noninvasive methods may be possible.

**Keywords**—Pulmonary arterial hypertension, PAH, Ventricular–vascular hemodynamic coupling, Cardiac Magnetic Resonance Imaging, Pulse pressure.

---

Address correspondence to Naomi C. Chesler, Department of Biomedical Engineering, University of Wisconsin-Madison, 2146 Engineering Centers Building, 1550 Engineering Drive, Madison, WI 53706-1609, USA. Electronic mail: chesler@engr.wisc.edu

## INTRODUCTION

Pulmonary arterial hypertension (PAH) is a devastating disease exhibiting fast progression<sup>14</sup> and poor prognosis.<sup>20,26</sup> PAH originates from increased resistance to blood flow in the small pulmonary arteries and arterioles. As a consequence of the increase in pressure, the proximal pulmonary arteries (PAs) become progressively stiffer and right ventricular (RV) function is impaired. In most PAH patients, RV failure is the direct cause of demise. The progression from pulmonary vascular pathology (increased resistance and reduced compliance) to RV dysfunction remains poorly understood.

RV function is typically assessed by measuring RV stroke volume (SV) and ejection fraction (EF), but those parameters do not provide sufficient insight into the RV response to pulmonary hypertension (PH). From a hemodynamic standpoint, efficiency and coupling of the ventricular–vascular system have been demonstrated to be sensitive to pulmonary vascular disease.<sup>16</sup> The parameter  $\eta_{VV}$ , which is the ratio of end systolic ventricular elastance  $E_{es}$  (a load independent measure of ventricle contractility) to effective arterial elastance  $E_a$  (a measure of the afterload), has been used to evaluate the efficiency of ventricular vascular coupling.<sup>28,29</sup> It is generally accepted that  $\eta_{VV}$  is larger than unity in healthy subjects<sup>16,22,30</sup>, whereas values of  $\eta_{VV}$  close to or lower than unity occur with disease.<sup>16,23,30</sup>

Novel approaches to investigate the pathologies of the right heart are leading to new metrics of RV function. Sanz *et al.*<sup>30</sup> assessed RV–PA coupling non-invasively using a simplified model that includes measurements from MRI only. Also, Das *et al.*<sup>15</sup> have

proposed that the efficiency of the RV can be estimated by the ratio of the net energy transferred to the blood pool in one heartbeat to the stroke work. This energy approach can be used along with  $\eta_{VV}$  to assess RV performance in PAH.

There is evidence that RV failure in PAH is correlated with the progressive stiffening of the large PAs. Increases in mean PA pressure (mPAP) and pulmonary vasculature resistance (PVR) are the primary parameters used in the diagnosis of PAH, but have limited prognostic value.<sup>2,11</sup> In contrast, decreases in total arterial compliance,<sup>25</sup> calculated as the stroke volume-to-pulse pressure ratio (SV/PP), and proximal PA relative area change (RAC)<sup>17</sup> are both correlated with mortality. These findings suggest that SV/PP and RAC may be correlated. Such a correlation, if proved, could be used to estimate PA pulse pressure (PP) from SV and RAC, both of which can be measured non-invasively by MRI. PP is an indicator of all-cause cardiovascular mortality and morbidity<sup>4</sup> and is correlated with mPAP.<sup>32</sup>

Large animal models of PAH can be used to evaluate the response of the right ventricular-pulmonary vascular system to a hypertensive state. Acute pulmonary embolism is one frequently used model<sup>18,21,33</sup> and has the advantage of the absence of long-term adaptation (remodeling) of the PAs and RV to the elevated mPAP. It is unclear whether RV dysfunction can be directly triggered by an acute increase in mPAP or if it also requires chronic changes in the RV and pulmonary vasculature. It has been reported that, similar to the left ventricle (LV),<sup>1,10,29</sup> the RV has a reserve of stroke work that can be used to compensate for acute increases in afterload, even quite significant increases.<sup>16</sup> However, the RV wall is thinner than the LV and so may be more susceptible to acute changes<sup>8</sup>; therefore, if even moderate hypertension is acutely induced by embolization, the RV is believed to have limited ability to compensate, which can quickly lead to RV failure.<sup>13</sup>

In this study we combine magnetic resonance imaging (MRI) and RHC to investigate the response of PA and RV to moderate, acute pulmonary embolization in healthy dogs. We assess RV volumes, RV-PA coupling efficiency and energy transfer ratio to clarify whether an acute increase in mPAP to over 30 mmHg is able to impair RV function and efficiency and cause decoupling. We also investigate the effect of increased mPAP on arterial stiffening, to ascertain whether SV/PP and RAC, which is strictly an area strain or deformability but correlates well with PA stiffness, are correlated in acute pulmonary embolism. Our hypotheses are (1) that an acute increase in peripheral resistance does not impair RV function, RV-PA coupling or energy transfer, and (2) in the absence of PA

remodeling, proximal PA stiffness (RAC) and total PA compliance (SV/PP) are correlated.

## MATERIALS AND METHODS

Acute PAH was induced by microbead injection in six female beagles ( $8.3 \pm 2.4$  kg body weight). The sequence of experimental procedures is outlined in Fig. 1.

General anesthesia was induced in all dogs by intravenous propofol injection (10 mg/kg body weight). After endotracheal intubation, anesthesia was maintained with isoflurane (1–3%) in 100% oxygen using mechanical ventilation at a respiratory frequency of 11 breaths/min. Lactated Ringer's solution was infused at a rate of 10 mL/kg/h. A femoral arterial catheter was inserted and systemic arterial pressure (SAP) and arterial blood gases were monitored. The femoral and external jugular veins were catheterized for RHC access, delivery of emboli, delivery of contrast for angiography and blood sampling. Thirty minutes after the stabilization of the animals, baseline

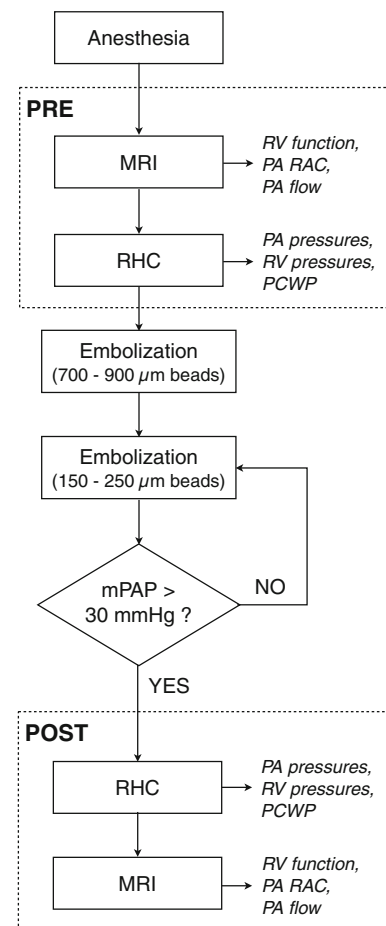


FIGURE 1. Flowchart of the experimental procedures.

CO, SAP, PAP (systolic, diastolic, mean), pulmonary capillary wedge pressure (PCWP), RV pressure, and right atrial pressure were measured.

While maintaining the dog under anesthesia, magnetic resonance imaging (MRI) and right heart catheterization (RHC) were repeated twice, first to obtain baseline vitals, pressures, RV function, and large PA geometry in the healthy animal (PRE tests), and second to measure the same parameters after acute PAH was successfully induced by embolization (POST tests). Dogs were humanely euthanized after the POST tests. All the procedures were approved by the Institutional Animal Care and Use Committee (IACUC) of the University of Wisconsin-Madison.

### Magnetic Resonance Imaging

MRI studies were performed on a clinical 3T scanner (MR750, GE Healthcare, Waukesha, WI, USA) using an 8-channel cardiac coil and vector electrocardiographic (ECG) gating. RV function was assessed from axial ECG-gated CINE balanced steady state free precession (SSFP) images through the entire heart. Parameters for SSFP imaging included:  $31 \times 19$  cm field of view,  $224 \times 192$  matrix, 7 mm slice, 0 mm gap,  $\pm 125$  kHz bandwidth, TR/TE = 3.1/1.1 ms (fractional readout), and segmentation factor of 12, for a true temporal resolution of 37 ms. Twenty interpolated time frames were reconstructed at each slice location. Between 13 and 16 slices were acquired depending on anatomy, each slice within an 8–10 s time interval of suspended ventilation.

2D phase contrast (PC) images were acquired in double oblique planes through the main PA (just distal to the pulmonic valve plane), the left and the right PA. Image parameters for 2D PC imaging were:  $35 \times 26$  cm field of view,  $256 \times 160$  matrix, 7 mm slice,  $\pm 62.5$  kHz bandwidth, 150 cm/s velocity encode (“venc”), TR/TE = 5.5/2.6 ms (full echo), and segmentation factor of 8, for a true temporal resolution of 44 ms. Twenty interpolated time frames were reconstructed. One slice was acquired while suspending ventilation for approximately 15–17 s.

### Right Heart Catheterization

Measurement of PAP (mean, systolic, and diastolic) and PCWP was performed with a fluid-filled pressure catheter advanced from the femoral vein into the main PA under fluoroscopic guidance. The pressure catheter was then withdrawn into the RV to measure end systolic pressure (RVESP) and end diastolic pressure (RVEDP). Pulmonary vasculature resistance (PVR) was calculated from pressure and flow data as follows:

$$PVR = \frac{mPAP - PCWP}{CO} \quad (1)$$

### Embolization

To create acute PH, polyvinyl alcohol microbeads (Contour SE Microspheres, Boston Scientific, Natick, MA, USA) were repeatedly injected into the right atrium through a catheter *via* the external jugular vein. A first increase in mPAP was obtained by injecting 2 mL of 700–900  $\mu$ m beads. Subsequently, 2–5 mL of 150–250  $\mu$ m beads were injected in multiple stages to gradually increase mPAP. PAP was measured intermittently and bead injection was continued until mPAP was greater than 30 mmHg (Fig. 1).

### Data Analysis

RV function was assessed analyzing the axial ECG-gated CINE balanced steady-state-free-precession (SSFP) images with ReportCard™ (GE Healthcare, Waukesha, WI, USA). Images were semi-automatically segmented to calculate RV volume at each of the 20 time frames during the cardiac cycle. End diastolic volume (EDV) and end systolic volume (ESV) were obtained as the minimum and maximum volumes, respectively. Stroke volume SV and ejection fraction EF were calculated as  $SV = EDV - ESV$  and  $EF = SV/EDV$ , respectively. Cardiac output (CO) was calculated as the product of SV and heart rate (HR).

In order to measure cross sectional area and blood flow in the main, left, and right PA, the 2D PC images were analyzed using the CV Flow analysis tool (Medis, Leiden, The Netherlands). The PA contours were segmented manually on the phase images to obtain blood velocity over the entire cardiac cycle and on the magnitude images to evaluate the cross sectional area at peak systole ( $A_{max}$ ) and at end diastole ( $A_{min}$ ). The relative area change (RAC) was calculated as:

$$RAC = \frac{A_{max} - A_{min}}{A_{max}} \quad (2)$$

Mean blood flow through the PA was calculated as the product of the average velocity and the cross sectional area at a given time during the cardiac cycle.

The end-systolic elastance  $E_{es}$  can be evaluated from pressure–volume loops using either multi-beat<sup>19</sup> or single-beat methods.<sup>6,33</sup> Single beat methods have been extensively used but their validity in the RV is still unclear.<sup>24</sup> In addition the choice of the portion of the original pressure waveform to use for the sinusoidal fit increases the uncertainty of  $P_{max}$  estimates. In this study we assumed that the volume-axis intercept of the ESPVR can be neglected<sup>12,30</sup> and so calculated the

end-systolic elastance as the maximal pressure/volume ratio in the RV<sup>9</sup>:

$$E_{es} = (P/V)_{\max} \quad (3)$$

The effective arterial elastance  $E_a$  was originally defined as a steady-state parameter that incorporates the principal elements of the Windkessel model of the pulmonary vascular bed. It has been shown that taking into account the left atrial pressure provides a better approximation of  $E_a$  than mPAP/SV.<sup>27</sup> We used PCWP as an approximation of the left atrial pressure and calculated  $E_a$  as:

$$E_a = \frac{\text{mPAP} - \text{PCWP}}{\text{SV}} \quad (4)$$

RV–PA coupling efficiency was calculated as  $\eta_{vv} = E_{es}/E_a$ . We also tested a simplified model proposed by Sanz *et al.*<sup>30</sup> proposed to evaluate the coupling efficiency from MRI data only:

$$\eta'_{vv} = \frac{SV}{ESV} \quad (5)$$

Pressure–volume loops, obtained by combining MRI and RHC data, were integrated to evaluate the stroke work (SW). PA pressure from RHC and flow data from 2D PC images also were combined to calculate  $E_{\text{net}}$  using the formulation proposed by Das *et al.*<sup>15</sup>:

$$E_{\text{net}} = \int_0^T \left( p + \frac{1}{2} \rho v^2 \right) Q dt \quad (6)$$

where  $p$ ,  $v$ , and  $Q$  are, respectively, time-dependent pressure, velocity, and flow rate in the main PA,  $\rho$  is blood density and  $T$  is the heartbeat duration.

From the hypothesis that the total arterial compliance SV/PP is correlated with the RAC, we formulated the following model to calculate PP from MRI measurements of SV and RAC:

$$\text{PP} = \frac{\text{SV}}{\alpha_{\text{PP}} \cdot \text{RAC} + \beta_{\text{PP}}} \quad (7)$$

A nonlinear regression was performed in MATLAB 7.12 (The Mathworks, Natick, MA, USA) to estimate the coefficients  $\alpha_{\text{PP}}$  and  $\beta_{\text{PP}}$ .

In order to formulate a model for mPAP, we determined the slope and intercept of the linear correlation between mPAP and PP,<sup>32</sup> and included the intercept ( $d_m$ ) as a constant in a nonlinear regression to estimate the coefficients  $\alpha_m$  and  $\beta_m$  in the correlation

$$\text{mPAP} = \frac{\text{SV}}{\alpha_m \cdot \text{RAC} + \beta_m} + d_m \quad (8)$$

We repeated the nonlinear regression for the sPAP:

$$\text{sPAP} = \frac{\text{SV}}{\alpha_s \cdot \text{RAC} + \beta_s} + d_s \quad (9)$$

where  $d_s$  is the intercept we calculated from the linear correlation between sPAP and PP.<sup>32</sup>

All the tests for one animal were performed on the same day and we verified that the heart rate during MR was less than 10% different from that during RHC. All data are reported as mean value  $\pm$  standard deviation. Statistical significance was investigated using a paired  $t$  test. A 2-tailed probability value  $p < 0.05$  was considered evidence of statistical difference. Values of  $p < 0.001$  were noted as highly significant. Agreement between RHC and MRI estimates of PP, mPAP, and sPAP were evaluated using the  $R^2$  correlation coefficient and the Bland–Altman plot.

## RESULTS

Table 1 summarizes the data obtained from RHC and MRI for the six dogs before (PRE) and after (POST) embolization. Embolization resulted in a dramatic increase of the pressure in the PA. Mean PAP increased by about three times ( $p < 0.001$ ) and PP also increased significantly ( $p = 0.047$ ). PVR was more than doubled after embolization ( $p = 0.002$ ). PCWP doubled ( $p = 0.001$ ), but the POST values were low enough ( $< 15$  mmHg) to exclude involvement of the left heart.<sup>3</sup>

After embolization, RV pressure was significantly larger at peak systole ( $p = 0.003$ ) as well as at end diastole ( $p = 0.006$ ).

### Right Ventricular Function

MRI measurements of RV function revealed no significant change in ESV or EDV. SV was maintained at an average value of  $\sim 15$  mL and EF did not change significantly. CO was also preserved after embolization ( $p = 0.330$ ). In order to maintain the RV function substantially unchanged in spite of the increased pulmonary arterial pressure, the RV produced a larger stroke work, which tripled from  $13.96 \pm 5.25$  mJ (PRE) to  $42.07 \pm 9.46$  mJ (POST) ( $p = 0.002$ ).

### Ventricular–Vascular Coupling and Energy Transfer Ratio

Pressure–volume data from RHC and MRI were used to evaluate the efficiency of RV–PA hemodynamic coupling. Table 2 summarizes the results of these calculations. After embolization,  $E_{es}$  nearly doubled ( $p = 0.033$ ) and  $E_a$  tripled ( $p = 0.005$ ). As a



**TABLE 1. Data from RHC and MRI for the six dogs before (PRE) and after (POST) embolization.**

Parameter	Technique	PRE	POST	<i>p</i> value
mPAP (mmHg)	RHC	13.00 ± 2.19	36.00 ± 8.74***	<0.001
sPAP (mmHg)	RHC	17.50 ± 2.51	48.67 ± 14.77*	0.003
dPAP (mmHg)	RHC	9.17 ± 2.86	28.50 ± 5.68***	<0.001
PP (mmHg)	RHC	8.33 ± 3.01	20.17 ± 9.56*	0.047
PCWP (mmHg)	RHC	5.00 ± 2.10	10.17 ± 1.47*	0.001
RVESP (mmHg)	RHC	18.67 ± 3.39	49.00 ± 13.49*	0.003
RVEDP (mmHg)	RHC	3.50 ± 1.38	7.33 ± 1.37*	0.006
PVR (Woods units)	RHC	6.39 ± 1.38	15.70 ± 4.07*	0.002
ESV (mL)	MRI	21.95 ± 11.19	24.76 ± 9.48	0.414
EDV (mL)	MRI	36.83 ± 13.12	39.43 ± 9.84	0.605
SV (mL)	MRI	14.88 ± 3.54	14.67 ± 2.91	0.912
EF %	MRI	42.96 ± 11.69	38.69 ± 10.91	0.215
CO (L/min)	MRI	1.18 ± 0.30	1.32 ± 0.36	0.330

mPAP, mean pulmonary arterial pressure; sPAP, systolic pulmonary arterial pressure; dPAP, diastolic pulmonary arterial pressure; PP, pulse pressure; PCWP, pulmonary capillary wedge pressure; RVESP, right ventricular end systolic pressure; RVEDV, right ventricular end diastolic volume; PVR, pulmonary vasculature resistance; ESV, end systolic volume; EDV, end diastolic volume; SV, stroke volume; EF, ejection fraction; CO, cardiac output.

\**p* < 0.05, \*\*\**p* < 0.001.

**TABLE 2. Contractility, afterload, coupling efficiency and RV performance calculated before (PRE) and after (POST) embolization.**

Parameter	Definition	PRE	POST	<i>p</i> value
$E_{es}$ (mmHg/mL)	$E_{es} = (P/V)_{max}$	1.54 ± 0.51	2.47 ± 0.91*	0.033
$E_a$ (mmHg/mL)	$E_a = (mPAP - PCWP)/SV$	0.55 ± 0.07	1.83 ± 0.68*	0.005
$\eta_{VV}$	$\eta_{VV} = E_{es}/E_a$	2.69 ± 0.95	1.37 ± 0.55*	0.009
$\eta'_{VV}$ (MRI)	$\eta'_{VV}$ (MRI) = SV/ESV	0.82 ± 0.36	0.69 ± 0.38	0.317
SW (mJ)		13.96 ± 5.25	42.07 ± 9.46*	0.002
$E_{net}$ (mJ)	$E_{net} = \int_0^T (\rho + 0.5\rho v^2) Q dt$	27.66 ± 5.40	63.10 ± 20.24*	0.007
$E_{net}/SW$		2.49 ± 1.91	1.59 ± 0.72	0.227

Primed coupling efficiency is calculated from MRI data only.<sup>30</sup>

$E_{es}$ , end systolic elastance;  $E_a$ , arterial elastance;  $\eta_{VV}$ , RV-PA hemodynamic coupling efficiency; SW, stroke work;  $E_{net}$  net energy transfer.

\**p* < 0.05, \*\*\**p* < 0.001.

result, the coupling efficiency  $\eta_{VV}$  decreased from  $2.69 \pm 0.95$  before embolization to  $1.37 \pm 0.55$  after embolization (*p* = 0.009).

The values of  $\eta'_{VV}$  calculated from MRI data only<sup>30</sup> using Eq. (5) were lower than  $\eta_{VV}$ . In fact  $\eta'_{VV}$  was lower than unity even before embolization, and the decrease after embolization was not significant (*p* = 0.317).

The net energy  $E_{net}$  transferred to blood was more than doubled after embolization (*p* = 0.007). The net energy transfer ratio  $E_{net}/SW$  was only moderately decreased (*p* = 0.227).

#### Pulmonary Artery Flow

Mean blood flow through the main PA did not change significantly from PRE to POST (*p* = 0.089). Flow was unevenly split between left and right PA, as shown in Fig. 2. The difference between left PA mean flow and right PA mean flow was significant before

embolization (*p* = 0.016) and even more significant after embolization (*p* = 0.004). The left-to-right flow ratio was reduced from  $0.70 \pm 0.20$  (PRE) to  $0.55 \pm 0.12$  (POST), although the change was not significant (*p* = 0.224).

#### Arterial Stiffening

The total arterial compliance, SV/PP, decreased from  $1.87 \pm 0.44$  mL/mmHg (PRE) to  $0.91 \pm 0.57$  mL/mmHg (POST) (*p* = 0.039). The relative area change (RAC) of the main, left, and right PA, as measured by 2D PC MRI, also decreased and differences between left and right PA were evident (Fig. 3). In the main PA, the RAC dropped from  $0.40 \pm 0.05$  (PRE) to  $0.25 \pm 0.08$  (POST) (*p* = 0.025). Similarly, the RAC was decreased in the left PA (*p* = 0.008). In contrast, the RAC of the right PA did not change significantly (*p* = 0.330).

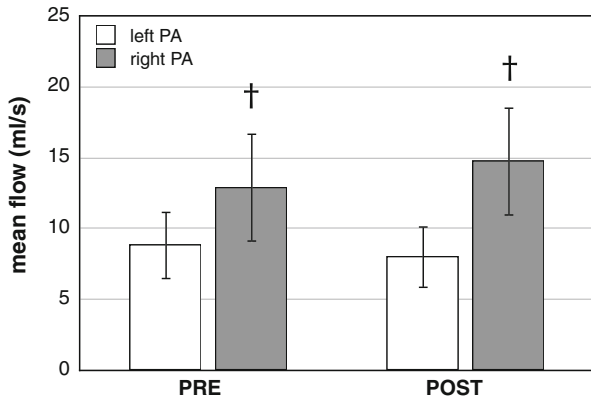


FIGURE 2. Mean blood flow through the left and right PA, before and after embolization ( $\dagger p < 0.05$  between left and right PA).

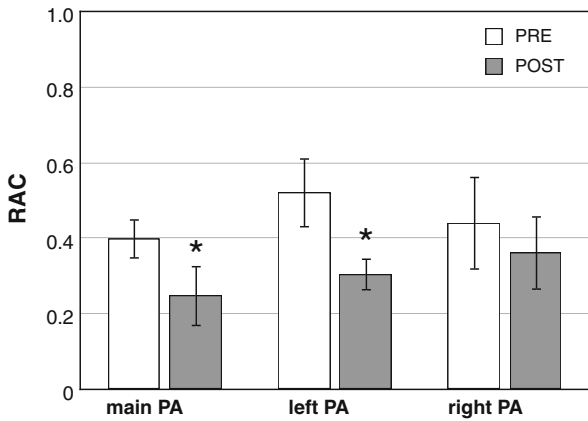


FIGURE 3. Relative area change (RAC) for the main, left, and right PA, before (PRE) and after (POST) embolization ( $*p < 0.05$ ,  $***p < 0.001$ ).

We correlated the total arterial compliance, SV/PP, with the RAC measured at a single location in each of the large PAs. The scatter plot in Fig. 4 shows that SV/PP has a strong correlation with the RAC calculated in the main PA ( $R^2 = 0.918$ ). We found poorer correlation with the RAC in the left PA ( $R^2 = 0.372$ ) and no correlation with the RAC in the right PA ( $R^2 = 0.004$ ).

We performed a nonlinear regression of the correlation for PP (Eq. 7), using the RAC measured in the main PA. The regression coefficients were estimated as  $\alpha_{PP} = 6.41$  mL/mmHg and  $\beta_{PP} = -0.705$  mL/mmHg. In Fig. 5a we plot  $PP_{MRI}$  vs.  $PP_{RHC}$  ( $R^2 = 0.965$ ). Figure 5b shows the Bland–Altman plot of the difference between  $PP_{MRI}$  and  $PP_{RHC}$ . The small bias and limits of agreement, along with the lack of any clear pattern or variance dependence on mean PP, indicate a good agreement between  $PP_{MRI}$  and  $PP_{RHC}$ .

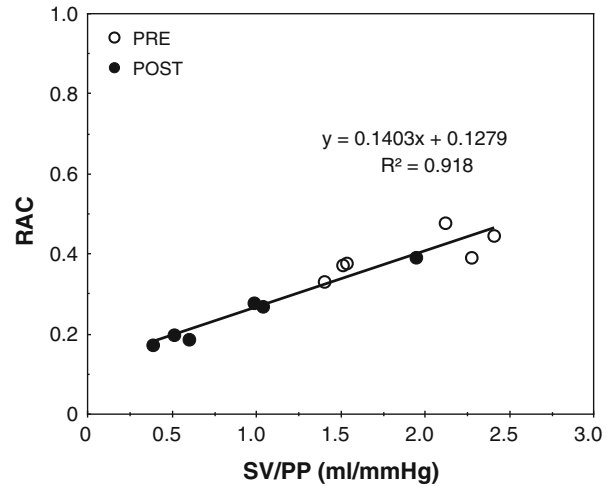


FIGURE 4. Relative area change (RAC) for the main PA, plotted as a function of SV/PP. Open and filled circles indicate PRE and POST embolization, respectively.

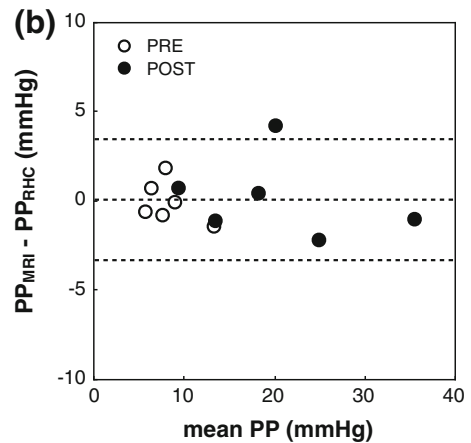
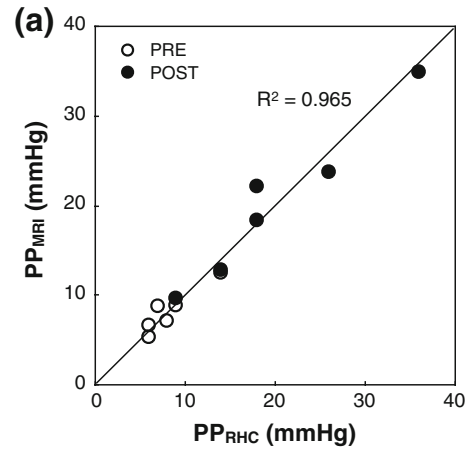


FIGURE 5. (a) Comparison of  $PP_{MRI}$  and  $PP_{RHC}$ . Line of equality is included. (b) Bland–Altman plot of the difference between  $PP_{MRI}$  and  $PP_{RHC}$ . The bias is 0.074 mmHg and the standard deviation is 1.72 mmHg, resulting in limits of agreement of  $-3.29$  and  $3.44$  mmHg (displayed as dashed lines). Open and filled circles indicate PRE and POST embolization, respectively.

The pulse pressure exhibited a good linear correlation with mPAP ( $R^2 = 0.775$ ) and a strong linear correlation with sPAP ( $R^2 = 0.888$ ). The intercepts of the linear correlations, required as inputs in Eqs. (8) and (9), were found to be  $d_m = 6.06$  mmHg and  $d_s = 5.00$  mmHg. From nonlinear regression of the correlation for mPAP (Eq. 8) we estimated  $\alpha_m = 4.65$  mL/mmHg and  $\beta_m = -0.486$  mL/mmHg. The correlation between mPAP<sub>MRI</sub> and mPAP<sub>RHC</sub> is shown in Fig. 6a ( $R^2 = 0.786$ ) and 6-B (Bland–Altman plot). Using the correlation for sPAP (Eq. 9), we estimated  $\alpha_s = 3.12$  mL/mmHg and  $\beta_s = -0.332$  mL/mmHg. The agreement between sPAP<sub>MRI</sub> and sPAP<sub>RHC</sub> (Figs. 6c, 6d) is similar to the results found for mPAP. The stronger correlation coefficient ( $R^2 = 0.887$ ) can be attributed to the wider range of sPAP values.

## DISCUSSION

The main finding of this study is that a near tripling of mPAP caused by acute embolization does not impair RV function or decouple the RV from the pulmonary vasculature. After embolization, stroke volume and ejection fraction were preserved and, in spite of the increase in afterload ( $E_a$ ), the RV increased its contractility ( $E_{es}$ ) sufficiently to prevent hemodynamic uncoupling. We found that the elastance ratio was decreased by about 50%, but remained in a range ( $1 < \eta_{vv} < 2$ ) where, according to theory, stroke work can be increased without significant impact on RV function.<sup>10</sup> These results are consistent with several previous investigations of acute embolization, which demonstrated preservation of RV function and

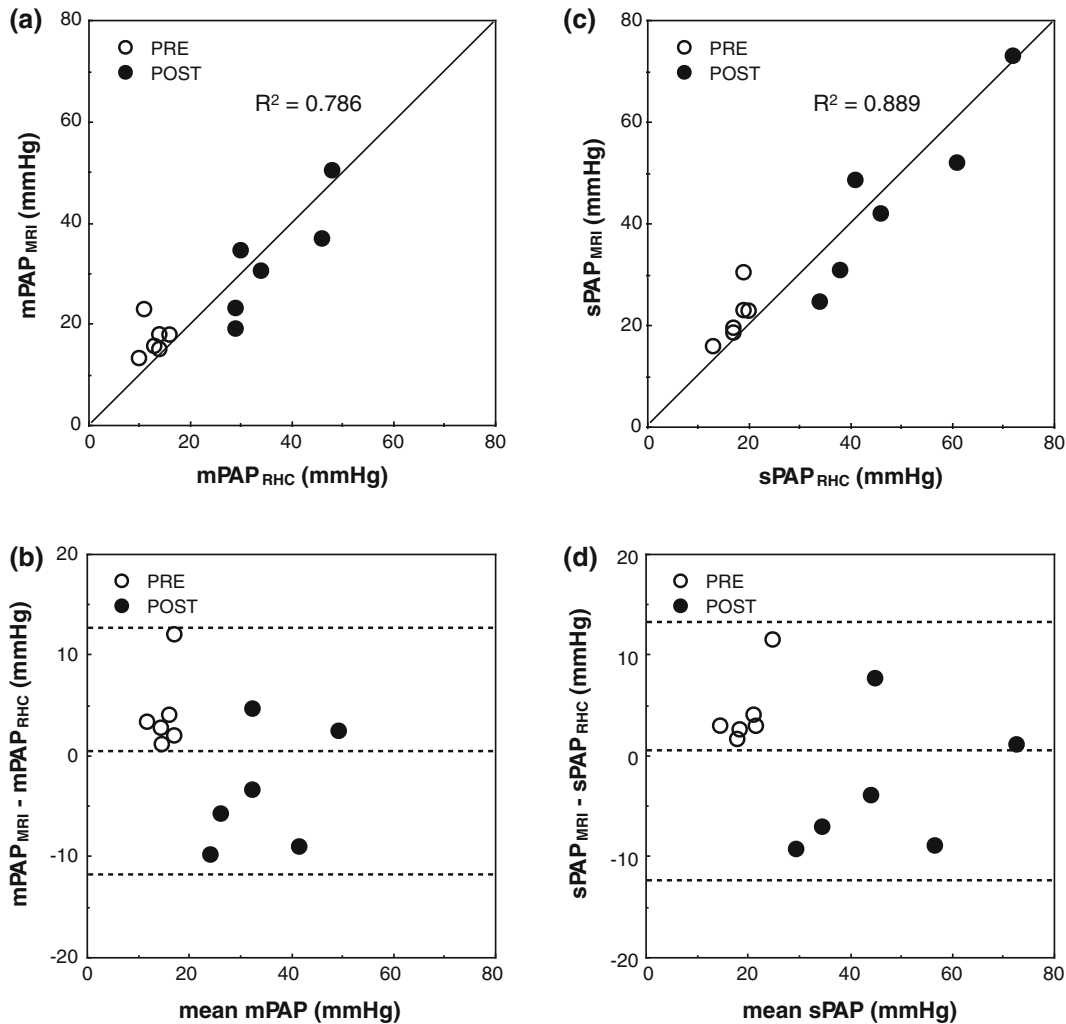


FIGURE 6. Comparison of mPAP (a) and sPAP (c) evaluated from MRI and RHC. Line of equality is included. Bland–Altman plot of the difference between MRI and RHC estimates of mPAP (b) and sPAP (d). For the mPAP the bias is 0.428 mmHg and the standard deviation is 6.28 mmHg, so the limits of agreement are  $-11.9$  and  $12.7$  mmHg (displayed as dashed lines). For the sPAP the bias is 0.502 mmHg and the standard deviation is 6.50 mmHg. The limits of agreement are  $-12.2$  and  $13.2$  mmHg (displayed as dashed lines). Open and filled circles indicate PRE and POST embolization, respectively.

RV–PA coupling in dogs and goats<sup>33</sup> and pigs.<sup>16,18</sup> In contrast with a recent study on acutely embolized pigs,<sup>21</sup> our study showed that adequate coupling is maintained when the mean pulmonary arterial pressure is nearly tripled.

Our results also demonstrate good agreement between the novel energy analysis proposed by Das *et al.*<sup>15</sup> and the elastance ratio method ( $\eta_{vv}$ ). While both the SW produced by the RV and the net energy  $E_{\text{net}}$  transferred to the blood flow increased after embolization, the ratio  $E_{\text{net}}/\text{SW}$  showed a 36% (non significant) decrease, similar to  $\eta_{vv}$ . Although  $E_{\text{net}}/\text{SW}$  is not strictly an efficiency (tissue elasticity and friction losses are not accounted for<sup>15</sup>), the moderate decrease observed here points to a potential reduction in the ability of RV to efficiently transfer energy to the blood pool. This approach to hemodynamic analysis also confirms our hypothesis that in acute PH the RV–PA system is able to preserve its functionality without uncoupling. To do so, the RV increases contractility and shifts towards maximum work at the expense of a modest reduction in efficiency.

We also tested a model proposed recently to assess the hemodynamic coupling efficiency from MRI measurements only.<sup>30</sup> The parameter  $\eta'_{vv}$  (Eq. 5) showed no significant change after embolization. However, it was lower than unity in both PRE and POST conditions, which according to the theory would imply a severe impairment of RV function even in the normotensive state. As this model clearly overestimates  $E_a$  (PCWP is neglected), the threshold value of  $\eta'_{vv}$  from healthy to failing RV may be lower than the generally accepted value  $\eta_{vv} = 1$ .

PA area strain (RAC) and total arterial compliance (SV/PP) were decreased after embolization. In the absence of arterial remodeling (wall thickening or alterations of the collagen content), acute stiffening was related to the pressure-induced stretching of the PAs. This mechanism can be quite different from the progressive loss of arterial compliance observed in chronic PH where long-term adaptation plays a major role. In future studies, comparing the characteristics of acute and chronic stiffening could provide new insight into the progression of the disease and the role of proximal PA function in mediating RV failure.

We demonstrated that total arterial compliance, SV/PP, has a strong linear correlation with the RAC in the main PA. The ratio SV/PP, although known to overestimate the true arterial compliance, has attracted large interest because of its simple formulation and excellent correlation with more accurate measures of arterial compliance.<sup>31</sup> Also, SV/PP is a strong predictor of mortality in PAH.<sup>25</sup> However, direct evaluation of SV/PP requires invasive measurement of pulse pressure in the PA. The RAC represents the PA area

strain, or relative deformation, and as such is not a measure of compliance. However, since sPAP and dPAP are linearly correlated,<sup>32</sup> the RAC is a valid surrogate of the local arterial stiffness coefficient  $\beta = \ln(\text{sPAP}/\text{dPAP})/(2\text{RAC})$  and can be obtained in a noninvasive fashion from MRI measurements at a single location in any of the extralobar PAs.

From the linear correlation between SV/PP and RAC, we developed an empirical correlation (Eq. 7) to assess PP non-invasively from MRI measurements of SV and RAC. Pulse pressure is a significant independent predictor of all-cause cardiovascular mortality,<sup>4</sup> although its prognostic value in PAH has been questioned.<sup>5</sup> Our analysis showed that values of PP estimated from MRI data are in excellent agreement with the measurements from RHC. Since we found that in moderate, acute pulmonary embolism SV is preserved, Eq. (7) demonstrates an inverse relationship between PP and RAC. Therefore, invasive measurement of PA pressures can be replaced with noninvasive assessment of RAC to monitor PA function in acute PH.

Taking advantage of the linear correlation of PP with mPAP and sPAP, we extended our analysis to formulate a model for noninvasive evaluation of mPAP and sPAP. For both parameters, the estimates based on MRI showed very little bias with respect to the RHC measurements and no clear pattern in the Bland–Altman plot, although the limits of agreement were broader than in the correlation proposed for  $\text{PP}_{\text{MRI}}$ .

This study has a number of limitations. RHC measurements of pressure and MRI measurements of volumes and flow were not performed simultaneously. However, all the tests for one animal were performed on the same day and we verified that the heart rate during MR was less than 10% different from that during RHC. To measure the end systolic elastance (Eq. 3) we assumed that the volume-axis intercept of the ESPVR could be neglected. Since we did not alter the RV preload, we could not verify the validity of that assumption, nor did we use a multiple beat assessment of  $E_{\text{es}}$ . We did not use the single beat method in this study, because its validity in the right heart has been questioned.<sup>7,24</sup> We believe that evaluating RV contractility without altering preload is still an unsolved problem.

The evaluations of the noninvasive estimates of PP, mPAP, and sPAP were based on a limited population in a single species. In addition, in acute embolization there is no remodeling of PA or RV and thus the arterial stiffening observed in our study is due to the stretching of the PA caused by pressure elevation as noted above. The linear correlation between total arterial compliance and local relative area change



might no longer be valid in the presence of significant arterial remodeling. Therefore further investigation will be necessary to test this approach in chronic PH and clinically.

Our results seem to indicate that embolization was unevenly distributed between the left and right sides of the pulmonary vasculature. This may be related to the poor correlation between total arterial compliance and the RAC measured in the right PA. Indeed, the RAC in the right PA did not exhibit a significant change from PRE to POST. We conjecture that, since the branching of the main PA presents a sharper change of direction for the blood flowing into the right PA, inertia could have produced a non-symmetric distribution of the emboli when they were injected from the right atrium. The result would have been a smaller increase in resistance in the right side of the pulmonary vasculature, which in turn could be responsible for the slight change in flow distribution after embolization (Fig. 2) as well for the modest decrease of RAC in the right PA. We speculate that if comparable embolization occurred in the left and right PA, the total arterial compliance would correlate with RAC in all three PA segments.

## CONCLUSIONS

Acute pulmonary embolization of healthy dogs induced a dramatic stiffening of the PA and led to increased stroke work. In response to this acute insult, the RV was able to shift its working condition to preserve function and hemodynamic coupling with the PA. The increase in stroke work required a reduction in RV efficiency. Comparison to a model of chronic embolization will help us identify the mechanisms by which PA remodeling impairs RV function. We found good correlation between SV/PP and RAC in the main and left PA, which we developed into empirical models to estimate PP, mPAP, and sPAP non-invasively from MRI measurements. The values of PP calculated with this correlation were in excellent agreement with PP from RHC. MRI estimates of mPAP and sPAP exhibited a good agreement with the RHC measurements. If confirmed in large animal models of chronic PAH and clinically, these results may be a significant advance towards noninvasive monitoring of PAH.

## ACKNOWLEDGMENTS

The authors gratefully acknowledge funding support from NIH 1R01HL105598 (NCC) and Department of Radiology (CJF).

## REFERENCES

- <sup>1</sup>Asanoi, H., S. Sasayama, and T. Kameyama. Ventricular-arterial coupling in normal and failing heart in humans. *Circ. Res.* 65(2):483–493, 1989.
- <sup>2</sup>Badano, L. P., C. Gingham, J. Easaw, D. Muraru, M. T. Grillo, P. Lancellotti, B. Pinamonti, G. Coghlan, M. P. Marra, B. A. Popescu, and S. De Vita. Right ventricle in pulmonary arterial hypertension: haemodynamics, structural changes, imaging, and proposal of a study protocol aimed to assess remodelling and treatment effects. *Eur. J. Echocardiogr.* 11(1):27–37, 2010.
- <sup>3</sup>Barst, R. J., M. McGoon, A. Torbicki, O. Sitbon, M. J. Krowka, H. Olschewski, and S. Gaine. Diagnosis and differential assessment of pulmonary arterial hypertension. *J. Am. Coll. Cardiol.* 43(12 Suppl S):40S–47S, 2004.
- <sup>4</sup>Benetos, A., M. Safar, A. Rudnicki, H. Smulyan, J. Richard, P. Ducimetière, and L. Guize. Pulse pressure: a predictor of long-term cardiovascular mortality in a French male population. *Hypertension* 30(6):1410–1415, 1997.
- <sup>5</sup>Blyth, K. G., R. Syed, J. Chalmers, J. E. Foster, T. Saba, R. Naeije, C. Melot, and A. J. Peacock. Pulmonary arterial pulse pressure and mortality in pulmonary arterial hypertension. *Respir. Med.* 101(12):2495–2501, 2007.
- <sup>6</sup>Brimioulle, S., P. Wauthy, P. Ewalenko, B. Rondelet, F. Vermeulen, F. Kerbaul, and R. Naeije. Single-beat estimation of right ventricular end-systolic pressure–volume relationship. *Am. J. Physiol. Heart Circ. Physiol.* 284(5):H1625–H1630, 2003.
- <sup>7</sup>Brimioulle, S., P. Wauthy, and R. Naeije. Single-Beat evaluation of right ventricular contractility. *Crit. Care Med.* 33(4):917–918, 2005.
- <sup>8</sup>Bristow, M. R., L. S. Zisman, B. D. Lowes, W. T. Abraham, D. B. Badesch, B. M. Groves, N. F. Voelkel, D. M. Lynch, and R. A. Quaife. The pressure-overloaded right ventricle in pulmonary hypertension. *Chest* 114(1 Supplement):101S–106S, 1998.
- <sup>9</sup>Brown, K. A., and R. V. Ditchey. Human right ventricular end-systolic pressure–volume relation defined by maximal elastance. *Circulation* 78(1):81–91, 1988.
- <sup>10</sup>Burkhoff, D., and K. Sagawa. Ventricular efficiency predicted by an analytical model. *Am. J. Physiol.* 250(6):R1021–R1027, 1986.
- <sup>11</sup>Champion, H. C., E. D. Michelakis, and P. M. Hassoun. Comprehensive invasive and noninvasive approach to the right ventricle-pulmonary circulation unit. *Circulation* 120(11):992–1007, 2009.
- <sup>12</sup>Chantler, P. D., E. G. Lakatta, and S. S. Najjar. Arterial-ventricular coupling: mechanistic insights into cardiovascular performance at rest and during exercise. *J. Appl. Physiol.* 105(4):1342–1351, 2008.
- <sup>13</sup>Chin, K. M., N. H. S. Kim, and L. J. Rubin. The right ventricle in pulmonary hypertension. *Coron. Artery Dis.* 16(1):13–18, 2005.
- <sup>14</sup>D'Alonzo, G. E., R. J. Barst, S. M. Ayres, E. H. Bergofsky, B. H. Brundage, K. M. Detre, A. P. Fishman, R. M. Goldring, B. M. Groves, and J. T. Kernis. Survival in patients with primary pulmonary hypertension. Results from a national prospective registry. *Ann. Intern. Med.* 115(5):343–349, 1991.
- <sup>15</sup>Das, A., R. K. Banerjee, and W. M. Gottliebson. Right ventricular inefficiency in repaired tetralogy of fallot: proof of concept for energy calculations from cardiac MRI data. *Ann. Biomed. Eng.* 38(12):3674–3687, 2010.

- <sup>16</sup>Fourie, P. R., A. R. Coetzee, and C. T. Bolliger. Pulmonary artery compliance: its role in right ventricular-arterial coupling. *Cardiovasc. Res.* 26(9):839–844, 1992.
- <sup>17</sup>Gan, C. T., J. Lankhaar, N. Westerhof, J. T. Marcus, A. Becker, J. W. R. Twisk, A. Boonstra, P. E. Postmus, and A. Vonk-Noordegraaf. Noninvasively assessed pulmonary artery stiffness predicts mortality in pulmonary arterial hypertension. *Chest* 132(6):1906–1912, 2007.
- <sup>18</sup>Ghuysen, A., B. Lambermont, P. Kolh, V. Tchana-Sato, D. Magis, P. Gerard, V. Mommens, N. Janssen, T. Desai, and V. D’Orio. Alteration of right ventricular-pulmonary vascular coupling in a porcine model of progressive pressure overloading. *Shock* 29(2):197–204, 2008.
- <sup>19</sup>Gupta, K. B., J. E. Bavaria, M. B. Ratcliffe, L. H. Edmunds, Jr., and D. K. Bogen. Measurement of end-systolic pressure–volume relations by intra-aortic balloon occlusion. *Circulation* 80(4):1016–1028, 1989.
- <sup>20</sup>Hyduk, A., J. B. Croft, C. Ayala, K. Zheng, Z. Zheng, and G. A. Mensah. Pulmonary hypertension surveillance—United States, 1980–2002. *MMWR Surveill. Summ.* 54(5):1–28, 2005.
- <sup>21</sup>Kerbaul, F., Y. By, V. Gariboldi, C. Mekkaoui, P. Fesler, F. Collart, S. Brimiouille, Y. Jammes, J. Ruf, and R. Guieu. Acute pulmonary embolism decreases adenosine plasma levels in anesthetized pigs. *ISRN Cardiol.* 2011:750301, 2011.
- <sup>22</sup>Kuehne, T., S. Yilmaz, P. Steendijk, P. Moore, M. Groenink, M. Saaed, O. Weber, C. B. Higgins, P. Ewert, E. Fleck, E. Nagel, I. Schulze-Neick, and P. Lange. Magnetic resonance imaging analysis of right ventricular pressure–volume loops. *Circulation* 110(14):2010–2016, 2004.
- <sup>23</sup>Lambermont, B., A. Ghuysen, P. Kolh, V. Tchana-Sato, P. Segers, P. Gerard, P. Morimont, D. Magis, J. Dogné, B. Masereel, and V. D’Orio. Effects of endotoxic shock on right ventricular systolic function and mechanical efficiency. *Cardiovasc. Res.* 59(2):412–418, 2003.
- <sup>24</sup>Lambermont, B., P. Segers, A. Ghuysen, V. Tchana-Sato, P. Morimont, J. Dogné, P. Kolh, P. Gerard, and V. D’Orio. Comparison between single-beat and multiple-beat methods for estimation of right ventricular contractility. *Crit. Care Med.* 32(9):1886–1890, 2004.
- <sup>25</sup>Mahapatra, S., R. A. Nishimura, P. Sorajja, S. Cha, and M. D. McGoon. Relationship of pulmonary arterial capacitance and mortality in idiopathic pulmonary arterial hypertension. *J. Am. Coll. Cardiol.* 47(4):799–803, 2006.
- <sup>26</sup>McLaughlin, V. V., S. L. Archer, D. B. Badesch, R. J. Barst, H. W. Farber, J. R. Lindner, M. A. Mathier, M. D. McGoon, M. H. Park, R. S. Rosenson, L. J. Rubin, V. F. Tapson, J. Varga, R. A. Harrington, J. L. Anderson, E. R. Bates, C. R. Bridges, M. J. Eisenberg, V. A. Ferrari, C. L. Grines, M. A. Hlatky, A. K. Jacobs, S. Kaul, R. C. Lichtenberg, J. R. Lindner, D. J. Moliterno, D. Mukherjee, G. M. Pohost, R. S. Rosenson, R. S. Schofield, S. J. Shubrooks, J. H. Stein, C. M. Tracy, H. H. Weitz, and D. J. Wesley. ACCF/AHA 2009 expert consensus document on pulmonary hypertension: a report of the American college of cardiology foundation task force on expert consensus documents and the American heart association: developed in collaboration with the American college of chest physicians, American thoracic society, inc., and the pulmonary hypertension association. *Circulation* 119(16):2250–2294, 2009.
- <sup>27</sup>Morimont, P., B. Lambermont, A. Ghuysen, P. Gerard, P. Kolh, P. Lancellotti, V. Tchana-Sato, T. Desai, and V. D’Orio. Effective arterial elastance as an index of pulmonary vascular load. *Am. J. Physiol. Heart Circ. Physiol.* 294(6):H2736–H2742, 2008.
- <sup>28</sup>Sagawa, K. The end-systolic pressure-volume relation of the ventricle: definition, modifications and clinical use. *Circulation* 63(6):1223–1227, 1981.
- <sup>29</sup>Sagawa, K., L. Maughan, H. Suga, and K. Sunagawa. *Cardiac Contraction and the Pressure–Volume Relationship*. New York: Oxford University Press, p. 480, 1988.
- <sup>30</sup>Sanz, J., A. Garcia-Alvarez, L. Fernandez-Friera, A. Nair, J. G. Mirelis, S. T. Sawit, S. Pinney, and V. Fuster. Right ventriculo-arterial coupling in pulmonary hypertension: a magnetic resonance study. *Heart* 98(3):238–243, 2012.
- <sup>31</sup>Segers, P., S. Brimiouille, N. Stergiopoulos, N. Westerhof, R. Naeije, M. Maggiorini, and P. Verdonck. Pulmonary arterial compliance in dogs and pigs: the three-element windkessel model revisited. *Am. J. Physiol.* 277(2):H725–H731, 1999.
- <sup>32</sup>Syyed, R., J. T. Reeves, D. Welsh, D. Raeside, M. K. Johnson, and A. J. Peacock. The relationship between the components of pulmonary artery pressure remains constant under all conditions in both health and disease. *Chest* 133(3):633–639, 2008.
- <sup>33</sup>Wauthy, P., A. Pagnamenta, F. Vassalli, R. Naeije, and S. Brimiouille. Right ventricular adaptation to pulmonary hypertension: an interspecies comparison. *Am. J. Physiol. Heart Circ. Physiol.* 286(4):H1441–H1447, 2004.